

by F. Seitz and D. Turnbull (Academic, New York, 1958), p. 353.

¹⁷J. T. Ritter, *J. Chem. Phys.* **53**, 3461 (1970).

¹⁸*Handbook of Mathematical Functions with Formulas, Graphs, and Mathematical Tables*, 3rd ed., Natl. Bur. Std. Appl. Math. Ser. 55, edited by M. Abramowitz and I. A. Stegun (U. S. GPO, Washington, D. C., 1965), pp. 928-935.

¹⁹*Formulae and Tables for Statistical Work*, edited by C. R. Rao, S. K. Mitra, and A. Matthai (Statistical Publishing Society, Calcutta, India, 1966).

²⁰G. F. Imbusch, W. M. Yen, A. L. Schawlow, D. E. McCumber, and M. D. Sturge, *Phys. Rev.* **133**, A1029 (1964).

²¹A. E. Hughes, *Proc. Phys. Soc. (London)* **87**, 535 (1966).

²²C. B. Pierce, *Phys. Rev.* **148**, 797 (1966).

²³Although Hughes's curves are densitometer traces, the experimental procedures followed were such that the results should be proportional to the absorption coefficient, or nearly so [A. E. Hughes (private communication)]. In any case, the quantitative significance of the experimental results is not of major importance for our primary purpose, which is to illustrate our computational approach.

²⁴A. M. Karo and J. R. Hardy, *Phys. Rev.* **141**, 696 (1966).

²⁵G. Raunio, L. Almqvist, and R. Stedman, *Phys. Rev.* **178**, 1496 (1969); J. R. D. Copley, R. W. MacPherson, and T. Timusk, *ibid.* **182**, 965 (1969).

²⁶J. E. Ralph and M. G. Townsend, *J. Phys. C* **3**, 8 (1970).

²⁷C. C. Klick, D. A. Patterson, and R. S. Knox, *Phys. Rev.* **133**, A1717 (1964).

Thermal Conductivity and Specific Heat of Noncrystalline Solids*

R. C. Zeller[†] and R. O. Pohl

Laboratory of Atomic and Solid State Physics, Cornell University, Ithaca, New York 14850

(Received 28 May 1971)

The thermal conductivity of vitreous SiO₂, Se, and silica- and germania-based glasses has been measured between 0.05 and 100°K. Comparison with earlier work on noncrystalline solids shows that they all have the same conductivity within a factor of 5 over the entire temperature range investigated, with the same characteristic plateau around 10°K, and that their conductivity varies as T^n , $n \sim 1.8$, below $T = 1^\circ\text{K}$. Furthermore, the average phonon mean free path is large by comparison with the phonon wavelength, about 10^{-4} cm at 2°K and decreasing as T^{-4} at larger T , suggesting a Rayleigh-type scattering mechanism. Such a mean free path can be quantitatively explained by approximating the glassy structure with that of a crystal in which every atom is displaced from its lattice site. Then every atom scatters like an interstitial atom, or—even simpler—like one that is missing at its regular lattice site, with a scattering cross section determined by the missing mass (isotopic defect). The specific heat of amorphous SiO₂, GeO₂, and Se has been found to vary as $AT + BT^3$ between 0.1 and 1°K, with $A = 10$ erg/g °K² to within a factor of 2. This departure from the Debye specific heat may be characteristic of the glassy state, as all earlier measurements of other glasses [polystyrene, glycerol, Lucite (PMMA)] indicate a similar anomaly. Its origin is not clear. Impurities or surface effects through adsorbed gases are unlikely because of the many samples and experimental techniques used in different laboratories. We have tried to attribute the anomaly to low-lying electronic states, motional states of ions, trapped atoms or large groups of atoms, or one-dimensional vibrations within a three-dimensional solid, so far without success. At the present time, the only independent evidence for these excitations appears to be in the low-temperature thermal conductivity at $T < 1^\circ\text{K}$ described above.

I. INTRODUCTION

The thermal conductivity of noncrystalline dielectric solids differs markedly from that of crystalline ones.^{1,2} As an example, Fig. 1 shows the conductivities of crystalline and vitreous silicon dioxide. In crystals, the conductivity increases with decreasing temperature because the anharmonic umklapp processes become less frequent, and hence the phonon mean free path increases. Eventually, the mean free path becomes comparable to the sample dimensions, and the conductivity goes through a maximum and then decreases as the

specific heat decreases.³ The conductivity of crystals depends very much on the material, and in addition any disturbance of the lattice periodicity lowers the conductivity in a sometimes very characteristic way, as shown in Fig. 1, for example.⁴ In noncrystalline solids, the conductivity is several orders of magnitude smaller than in crystals, it decreases monotonically with decreasing temperature, and furthermore it is independent of the chemical composition: In Fig. 2, the conductivity of vitreous silica^{2,5-7} is compared with that of silica-based glasses containing large amounts of other oxides.^{2,8-13} The conductivities are practically

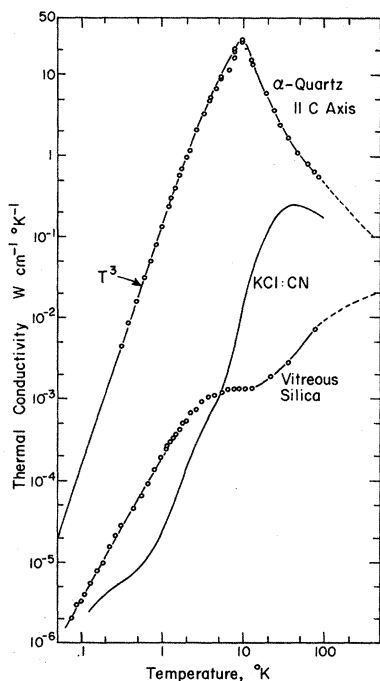


FIG. 1. Thermal conductivity of crystalline and of vitreous SiO_2 and of crystalline KCl:CN ($n_{\text{CN}} = 4.9 \times 10^{19} \text{ cm}^{-3}$). Sample dimensions: $5 \times 5 \times 40$ mm, sandblasted surfaces. Heatflow parallel to c axis in the quartz sample. The data above 100°K for quartz after Eucken (Ref. 1) and for vitreous silica after Ratcliffe (Ref. 6). Note that an impurity concentration of order 0.1% in the KCl crystal results in a conductivity smaller than that of the glass (the conductivity of pure KCl is similar to that of quartz). In KCl:CN, the low conductivity is caused by resonance scattering of the phonons by quasirotational states with energies close to 1.6 and 18 cm^{-1} (0.13×10^{-3} and $1.4 \times 10^{-3} \text{ eV}$) (Ref. 4).

identical. Even noncrystalline solids with completely different chemical compositions, such as polymers,¹⁴⁻¹⁷ varnishes,¹⁸ Se,¹² and GeO_2 ,¹⁹ all have very similar conductivities (Fig. 3).

The only exceptions appear to be glass ceramics^{10,20} such as Pyroceram, and the partially crystallizing polymers, such as nylon and Teflon^{9,14,21,22} and polyethylene.²³ Their conductivities are considerably smaller below 1°K than those of the noncrystalline solids, they depend on the sample, and they usually vary more rapidly with temperature.²⁴ The dependence of the conductivity on the crystallinity of polyethylene has been studied by Salinger.²³

The complete lack of sensitivity to composition in the noncrystalline solids would be understandable if the conductivity were as low as it could possibly be, corresponding to a diffusion of the vibrational energy from one atom to the neighboring ones. But this is not the case. A crystal containing as few as 0.1% of foreign ions can have a conductivity lower than that of the glasses (see Fig. 1). If an average

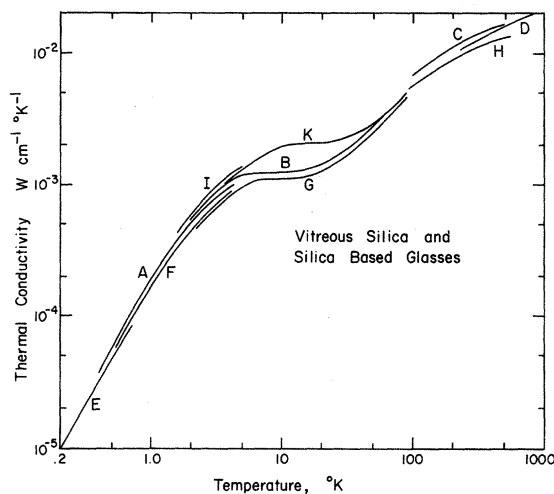


FIG. 2. Thermal conductivity of vitreous silica and silica-based glasses. Vitreous silica: A (Ref. 5), B (Ref. 2), C (Ref. 6), and D (Ref. 7). Borosilicate glasses, such as Pyrex (approximate composition by weight: 80% SiO_2 , 13% B_2O_3 , 4% Na_2O , 2% Al_2O_3 , 0.4% K_2O , 0.2% Li_2O): E (Ref. 9), F (Ref. 8), G (Ref. 2), and H (Ref. 13). Crown glass (unspecified composition): I (Ref. 10). "Soft" soda-lime glass (approximate composition: 70% SiO_2 , 15% Na_2O , and 10% CaO): K (Refs. 11 and 12). A summary of the chemical composition of glasses can be found in Ref. 6.

phonon mean free path l is defined by

$$K = \frac{1}{3} C_v v l, \quad (1)$$

where K is the thermal conductivity, C_v the specific heat of the plane lattice waves, and v the Debye sound velocity, l at 1°K is found to be of order 10^{-3} cm in glasses, i. e., 100 times the wavelength of the domi-

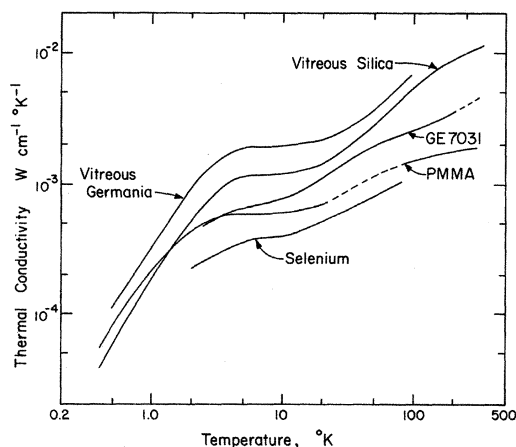


FIG. 3. Comparison of the thermal conductivity of vitreous silica with that of the polymer PMMA (Refs. 14-17) solid varnish (GE 7031) (Ref. 18), vitreous selenium (Ref. 12), and vitreous GeO_2 (germania) (Ref. 19). The curve for silica is a composite curve after Fig. 2.

nant lattice vibrations or 10^4 intermolecular spacings. Only at the highest temperatures, where glasses and crystals have approximately equal conductivities, is l of the order of the intermolecular spacing, i. e., 10^{-7} cm.²⁵ We will return to this point later in Fig. 9. Consequently, the problem has to be stated as follows: Why do all noncrystalline solids have the same (high) conductivity at low temperatures, and why do all the curves have the same characteristic shape with a plateau in the neighborhood of 10°K ? This question was the starting point for the present investigation.

Two models have been suggested to explain the conductivity of glasses. In the first model, Klemens²⁶ proposed that the scattering is caused by spatial fluctuations in the sound velocity and by a certain amount of long-range order and that this affects the transverse phonons more than the longitudinal ones. At temperatures below the plateau (10°K), the heat is mainly carried by longitudinal phonons, which are uncoupled from the transverse phonons. At around 10°K , the onset of the anharmonic interaction couples the phonons in the different branches and hence lowers the mean free path of the longitudinal phonons, which causes the plateau. Eventually, the conductivity increases again because the specific heat increases. As an alternative model, Klemens²⁷ proposed that in noncrystalline solids the heat carrying plane-wave phonons are resonantly scattered by localized phonons in a way similar to the resonant scattering found in crystals containing substitutional molecules with low-frequency quasirotranslational degrees of freedom (see Fig. 1) or in crystals containing defects causing resonant modes.²⁸ Such a scattering, in particular, could explain the plateau occurring in the temperature region in which most of the heat is carried by phonons whose frequencies are close to those of the spatially localized modes. These modes should be observable in the specific heat of glasses. It is known that the low-temperature specific heat of the same substance in the glassy phase is larger than that in the crystalline phase.²⁴ This has been observed in SiO_2 ,²⁹⁻³⁵ B_2O_3 ,³⁶ Se,³⁷⁻³⁹ glycerol,^{31,32,40} and polyethylene.⁴¹ As an example, we show in Fig. 4 the specific heats of SiO_2 in the vitreous and in the crystalline phase (α -quartz) plotted as $C_v T^{-3}$ vs T . The specific heats of the two phases of SiO_2 calculated in the Debye limit from elastic measurements are very similar. Therefore, the difference between the vitreous and crystalline specific heat has often been referred to as an excess specific heat and has been associated with some extra modes characteristic for the glassy phase. Dreyfus, Fernandes, and Maynard⁴² have suggested that these modes could be the localized modes responsible for the resonance scattering in the glassy phase. This

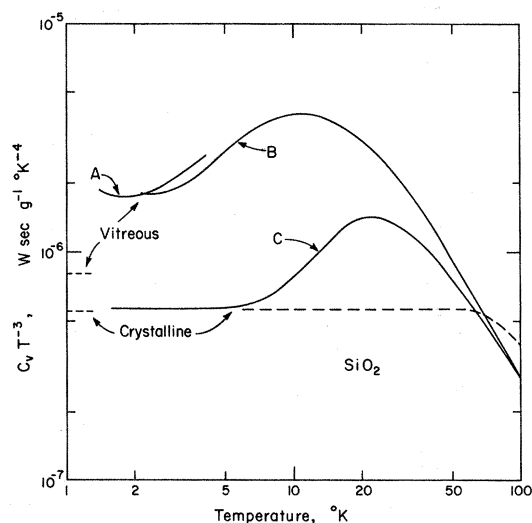


FIG. 4. Specific heat of vitreous SiO_2 and crystal quartz, plotted as $C_v T^{-3}$ vs T . A: I. R. Vitreosil (Ref. 29); B: vitreous silica (after Refs. 30–32); C: α -quartz (after Refs. 29, 33, and 34). The two short dashed lines indicate the specific heats calculated from elastic measurements: For vitreous silica, $C_{v,el} = 8.07 \times 10^{-7}$ ($\text{W sec g}^{-1} \text{K}^{-4}$) T^3 , calculated from $v_{av,el} = 4.1 \times 10^5$ cm sec^{-1} (Ref. 25). For crystal quartz $C_{v,el} = 5.5 \times 10^{-7}$ ($\text{W sec g}^{-1} \text{K}^{-4}$) T^3 , calculated from $v_{av,el} = 4.4 \times 10^5$ cm sec^{-1} (Ref. 35). See also Table I. The dashed curve shows $C_v T^{-3}$ for quartz in the Debye approximation for a Debye temperature of 552°K (based on the number density of atoms in the quartz).

model has also been applied to Se⁴³ and GeO_2 ,⁴⁴ and it has been concluded that the frequencies needed to explain the phonon scattering do agree with the frequencies of these excess modes.

Both the structure scattering and the localized mode scattering do not give a plausible reason for a particularly important experimental fact, namely, that all noncrystalline solids have practically identical thermal conductivities. This fact suggests that the scattering must have a very simple origin, extremely independent of structural details or the vibrational spectrum of the solids.

We end our introduction by pointing out a most peculiar fact demonstrated in Fig. 4: At the lowest temperatures investigated, there is no sign that the specific heat of the vitreous silica approaches that computed from elastic measurements in the Debye approximation. Instead, in both samples seems to be an indication of an upturn beginning below 2°K . This behavior appears not to be restricted to SiO_2 , as shown in Fig. 5 for the polymers polystyrene (PS) and polymethylmethacrylate (PMMA),⁴⁵ for glycerol,⁴⁶ and for vitreous GeO_2 .⁴⁷

The purpose of this paper is threefold:

(a) To present an extension of thermal conductivity measurements on noncrystalline solids to different materials and to even lower temperatures,

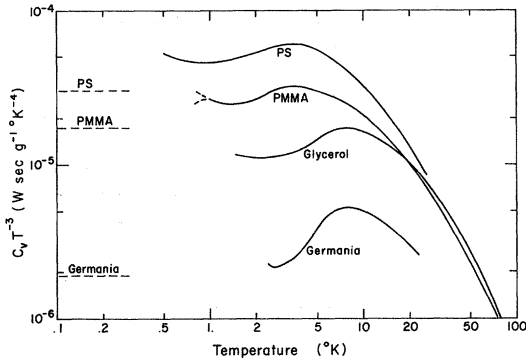


FIG. 5. Specific heat of several amorphous materials plotted as C_v/T^3 vs T : PS and PMMA (after Ref. 45), glassy glycerol (after Refs. 31, 32, 40 and 46), and vitreous germania (after Ref. 47). The dashed lines represent the low-temperature specific heat calculated from the sound velocities. There is some experimental uncertainty in the data on PMMA, indicated by the two short dashed lines.

in order to further demonstrate the striking independence of the material.

(b) To suggest a model which can quantitatively explain the thermal conductivity in the temperature range from a few degree Kelvin on up, and to test this model on three different substances.

(c) To show that the specific heat of noncrystalline solids below 1 °K does not follow the expected Debye T^3 law, but instead approaches a linear variation with temperature. This striking behavior seems to be characteristic for noncrystalline solids, and to be independent of accidental impurities. This anomaly may also be responsible for the thermal conductivity below 1 °K. Its origin is yet unknown.

II. EXPERIMENTAL METHODS

Thermal conductivity was measured with the steady-state method in cryostats designed to span the temperature range 0.05–100 °K. Specific heat was measured with the transient heating technique described earlier.^{4,48} For this, the sample was in thermal contact with the heat sink through a heat leak. After a heat pulse has been applied to the sample through an electrical heater (25- μ -diam nichrome, 50 cm long, glued to the sample with GE 7031 varnish), the initial temperature increase of the samples decayed exponentially through the heat leak. The time constant τ_{sb} of this cooling had to be large compared to the duration of the pulse and to any time constant associated with thermal equilibrium within the sample and between sample and heater or thermometer (a piece of a 220- Ω Speer resistor). The heat leak consisted of a 50- μ -thick copper wire or a short piece of 1-mm-diam graphite rod fastened with Epoxy to a thin copper

foil glued to the sample or to an evaporated gold film. Through the proper choice of the various components of this heat leak we obtained the sample to bath time constants shown in Fig. 6. Heat pulse duration was varied between 0.5 and 2 sec. The time constants for the thermal equilibration between heater and thermometer and the sample was always found to be less than 1 sec, the time constant of the Wheatstone bridge used to measure the temperature.⁴ The time constant τ for thermal equilibrium within the sample was estimated from the heat diffusion equation to be

$$\tau = C_v m d^2 / K, \quad (2)$$

where $C_v m$ and K are the heat capacity and thermal conductivity of the sample, respectively, and d is a characteristic length, typically a diameter of the sample.⁴⁹ For the noncrystalline samples used in this investigation, this τ was less than 0.1 sec at the lowest temperatures, and increased to approximately 1 sec at 1 °K. For the crystals, τ was even shorter. The largest source of error was random building vibrations transmitted to the sample, causing random temperature fluctuations and hence uncertainties in the determination of the sample temperature while the sample temperature returned to that of the bath following a heat pulse. These fluctuations caused a maximum error of 20% in the specific heat below 0.1 °K, but were negligible above 0.2 °K. As a test of our technique, we measured the specific heat C_v of single crystal RbBr and SiO₂ (Fig. 7). Our results are in good agreement with earlier data (RbBr, Rollefson *et al.*,⁵⁰ $T > 0.2$ °K; quartz, White and Birch,²⁹

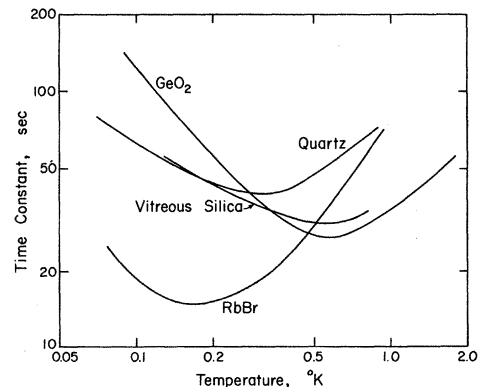


FIG. 6. Some of the experimental time constants τ_{sb} with which the temperature of the sample returned to that of the bath after the sample had been heated for a short time (~ 1 sec) with a known energy. Excitations which have relaxation times larger than τ_{sb} will remain unnoticed in this kind of experiment. We did not find that our results depended on the τ_{sb} chosen. We conclude that all time constants associated with thermal equilibration within the sample were much shorter than τ_{sb} (see text).

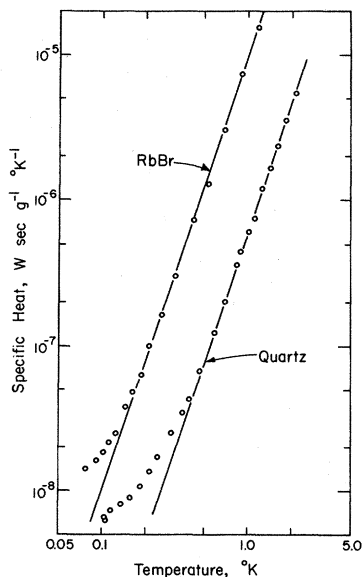


FIG. 7. Specific heat of RbBr and quartz. The solid lines, $C_{v,RbBr} = 9.7 \times 10^{-6} (\text{W sec g}^{-1} \text{°K}^{-4}) T^3$ and $C_{v,quartz} = 5.7 \times 10^{-7} (\text{W sec g}^{-1} \text{°K}^{-4}) T^3$ agree with those calculated from elastic measurements, and in the temperature range of overlap, also with earlier specific-heat measurements (RbBr, $T > 0.2 \text{°K}$, Ref. 50, quartz, $T > 1.4 \text{°K}$, Ref. 29).

$T > 1.4 \text{°K}$). At the lowest temperatures, below 0.15°K in RbBr and below 0.4°K in quartz, C_v ceases to vary as T^3 . For alkali halides, such an anomaly is known (NaF,⁵¹ KCl,⁴⁸ NaBr,⁵² RbCl⁵⁰) and has been shown to decrease with increasing pur-

ity of the samples. The anomaly has been attributed to tunneling impurities,⁵³ present even in the purest crystals in concentrations below the 1-ppm level. A similar anomaly in Al_2O_3 occurring around 10°K has been explained with low-energy spin states of impurities.⁵⁴ Although we have not yet investigated whether the anomaly in RbBr and in quartz is indeed caused by similar impurities, we assume that it will be absent in perfect crystals. In any event, this anomaly is over ten times smaller than the specific heat we will be concerned with in glasses.

Thermal conductivity was measured on natural quartz (Valpey Corp.) on pieces of vitreous silica (GE 201) and Pyrex (Corning 7740) and on a piece of selenium stringsawed from the specific-heat boule described below. Sample dimensions were approximately $5 \times 5 \times 40 \text{ mm}$; the surfaces were sandblasted. Also measured was a piece of aluminogermanate (Corning 9754) with the following composition (by weight): GeO_2 50%, Al_2O_3 25%, CaO 15%, BaO 5%, and Zn 5%.⁵⁵

The specific-heat samples used are listed in Table I. The quartz was natural material, Spectrosil B was synthetic silica, which according to its manufacturer contained a total of about 0.1 ppm of metallic impurities and 0.1% weight of hydroxyl (see below, caption of Fig. 13). A chemical analysis of the Pyrex samples⁵⁶ revealed iron concentrations of $2.3 \times 10^{18} \text{ cm}^{-3}$ (100 ppm) in the Pyrex 7740 and $2.9 \times 10^{17} \text{ cm}^{-3}$ (12 ppm) in the Pyrex 9700. The selenium sample was outgassed and melted in a

TABLE I. Specific-heat samples used in this investigation. Also listed is room-temperature mass density, molecular weight, and the 0°K Debye sound velocity v_D as calculated from elastic measurements, except for Se (see footnote f).

| Material | Supplier | Mass (g) | Temp. range (°K) | Mass density (g cm^{-3}) | Molec. weight | v_D (10^5 cm sec^{-1}) |
|-------------------------|----------------------|----------|------------------|-------------------------------------|---------------|--------------------------------------|
| α -quartz | Valpey | 44.0 | 0.8–2.0 | 2.6 | 60.09 | 4.4 ^a |
| α -quartz | Valpey | 122.9 | 0.1–0.9 | | | |
| Spectrosil B | Thermal American | 29.0 | 0.3–2.0 | 2.2 | 60.09 | 4.1 ^a |
| Spectrosil B | Thermal American | 110.0 | 0.13–0.8 | | | |
| Pyrex 7740 ^b | Corning | 43.0 | 0.3–2.0 | | | 3.65 ^c |
| Pyrex 9700 ^d | Corning | 46.0 | 0.3–2.0 | | | |
| Vitr. Se | Xerox ^e | 53.6 | 0.1–1.5 | 4.25 | 78.96 | 1.54 ^f |
| Vitr. GeO_2 | Cornell | 57.3 | 0.08–1.8 | 3.6 | 104.6 | 2.6 ^g |
| RbBr (cryst.) | Cornell ^h | 39.7 | 0.08–1.2 | 3.43 ⁱ | 165.4 | 1.59 ⁱ |

^aAfter Ref. 35.

^bApproximate composition (by weight): SiO_2 80.5%, B_2O_3 12.9%, Na_2O 3.8%, Al_2O_3 2.2%, K_2O 0.4%, and Li_2O 0.2%.

^cAfter W. P. Mason, in *American Institute of Physics Handbook* (McGraw-Hill, New York, 1963), pp. 3–88. Extrapolated to 0°K .

^dApproximate composition (by weight): SiO_2 80%, B_2O_3 13%, Na_2O 5%, and Al_2O_3 2%. This sample was kindly supplied by Dr. A. A. Erikson, Corning Research Laboratory.

^eSample kindly supplied by Dr. Mark Myers, Xerox Research Laboratory.

^fSince elastic data were unavailable, the value listed was calculated from the specific heat of the crystalline phase, see I. C. Lasjaunias, *Compt. Rend.* **B269**, 763 (1969).

^gAfter Ref. 47.

^hSame sample as the one studied in Ref. 50.

ⁱAfter J. T. Lewis, A. Lehoczyk, and C. V. Briscoe, *Phys. Rev.* **161**, 877 (1967). Mass density quoted is the one at 4°K .

quartz tube and quenched in air after melting.⁵⁷ The germania sample was melted at 1250 °C in vacuum in a Pt crucible, kept at that temperature for 18 h in oxygen at 1 atm, rapidly cooled to 600 °C and then slowly to room temperature. The sample showed an absorption with a maximum absorption constant $k = 15 \text{ cm}^{-1}$ at 2450 Å. This defect is associated with an oxygen deficiency (F' center).⁵⁸ Using Smakula's equation and assuming an oscillator strength $f = 1$,⁵⁹ we determined a defect concentration of $1 \times 10^{17} \text{ cm}^{-3}$ (5 ppm).

The simplest way to analyze thermal conductivity data is in the dominant-phonon approximation. In this approximation, one assumes that the heat is carried exclusively by those phonons which contribute most to the specific heat at that temperature, i. e., those phonons for which $dC_v/d\omega$ is a maximum. In the Debye approximation, the angular frequency ω_{dom} of the dominant phonons is $5.65 \times 10^{11} \text{ rad sec}^{-1}$ (3 cm^{-1} in the wave-number measure) at 1 °K and is proportional to the temperature. Thus, if C_v and v are known, $l(\omega_{\text{dom}})$ can be determined from the experiment with the help of Eq. (1). A simple estimate of the error to be expected if this method is used to determine the frequency dependence of the phonon mean free path was made as follows: The phonon scattering rates $\tau_{\text{iso}}^{-1}(\omega)$ resulting from isotopic mixtures in crystals are known both from theory²⁶ and experiment.⁶⁰ We analyzed the thermal conductivity data obtained on Ge crystals of different isotopic composition⁶¹ with the dominant-phonon approximation and obtained a relaxation rate $\tau_{\text{iso}}^{-1}(\omega_{\text{dom}})$ which varied as the fourth power of frequency and which differed from the theoretically predicted rate²⁶ $\tau_{\text{iso}}^{-1}(\omega)$ by less than a factor of 2. Another test for the validity of the dominant-phonon approximation, involving phonon resonance scattering, was performed by Narayanamurti and Pohl.⁵³

III. EXPERIMENTAL RESULTS AND DISCUSSION

A. Thermal Conductivity

The thermal conductivities of vitreous and crystalline SiO_2 measured in this investigation have been compared in Fig. 1. In Fig. 8 we compare the conductivities of several vitreous materials. As we pointed out in the introduction, all noncrystalline materials have practically identical conductivities. This is confirmed by our measurements. Our data, which extend to lower temperatures, show that the conductivities vary as T^n with $n \sim 1.8$, below 1 °K. The mean free paths, determined for quartz, vitreous silica, germania,¹⁹ and selenium with the help of Eq. (1) in the dominant-phonon approximation, are compared in Fig. 9. The specific heat used for this analysis was that of the crystal phase, except for GeO_2 , for which the specific heat is available only for the glassy phase.⁴⁷ The error

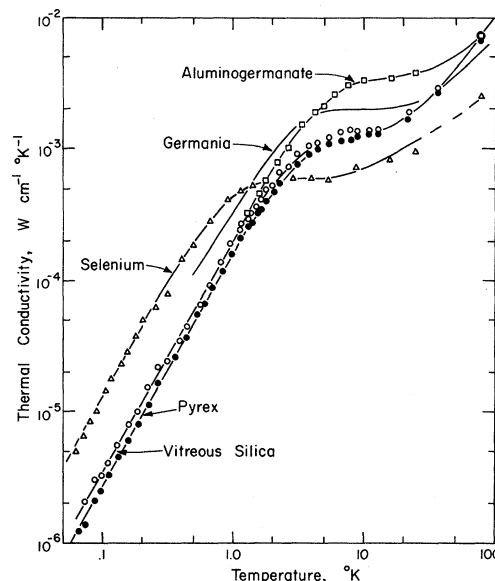


FIG. 8. Thermal conductivity of vitreous silica, Pyrex 7740, and selenium between 0.06 and 100 °K and of aluminogermanate glass between 1 and 100 °K. For comparison included is the conductivity of vitreous GeO_2 (Fig. 3 and Ref. 19). Our data on vitreous silica and on Pyrex 7740 agree closely with those obtained by Berman (Ref. 2). The data on Se are twice as large as those reported in Ref. 12. As far as we know, this is the only case where the conductivity of a noncrystalline solid has been found to be sample dependent. This difference may result from a difference in sample preparation: White *et al.* (Ref. 12) quenched their sample in water; our sample was cooled in air.

possibly introduced by not using the vitreous specific heats will be discussed below, but it is negligible for the present discussion, which deals with temperatures above 1 °K. The sound velocities used were the ones listed in Table I. At high temperatures, the mean free paths for crystalline and vitreous materials alike approach the order of a few angstrom, i. e., the interatomic separation, as is to be expected. As the temperature decreases, the mean free path increases very rapidly (almost exponentially) in the crystal. The mean free paths in the vitreous samples also increase, although not as rapidly, and with no sign of a resonance scattering process. In the region around 10 °K, the mean free path in these samples varies approximately as the fourth power of the temperature, or in the dominant-phonon approximation,

$$l(\omega_{\text{dom}}) \propto \omega_{\text{dom}}^{-4}, \quad (3)$$

reminding us of a Rayleigh scattering process. Static point defects, such as foreign atoms, vacancies, interstitial atoms, or isotopes in crystal lattices, cause such phonon scattering.²⁶

We attempt to explain the observed mean free

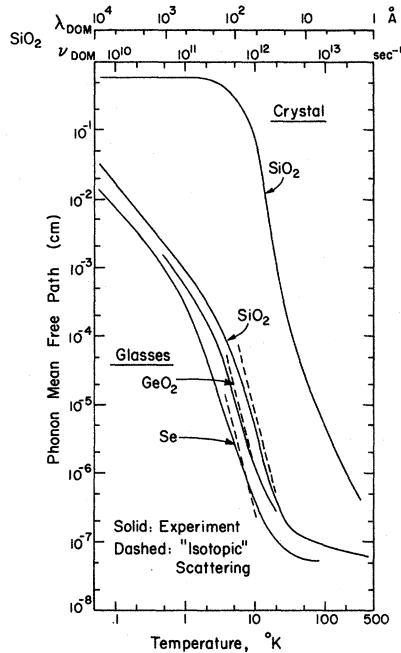


FIG. 9. Average phonon mean free path $l(T)$ after Eq. (1) for quartz and for vitreous SiO_2 , GeO_2 , and Se. Specific heats used for the evaluation of $l(T)$ was that of crystal quartz (Refs. 25, 29, and 30), vitreous GeO_2 (Ref. 47), extrapolated below 2 °K with the help of the Debye model (Fig. 5), and crystal Se (Ref. 39). Sound velocities used are listed in Table I. The dashed lines are theoretical values for the phonon mean free paths calculated from our "isotopic" scattering model. At the top of the figure are indicated the phonon wavelengths and frequencies for SiO_2 (both vitreous and crystalline) in the dominant-phonon approximation.

paths in the noncrystalline systems with the following model: We view these solids as *crystals*, in which every atom (or molecule) is displaced from its crystal lattice site by a random amount and in a random direction. It sits somewhere on an interstitial site. Hence, the solid consists of as many interstitial atoms as there are atoms in the solid. Because of the random displacement, the total scattering rate of these interstitial atoms will be given by the sum of the scattering rates of the individual atoms. This is similar to the phonon scattering by the random mass fluctuations in an isotopically mixed crystal: In the most general case, no atom has a mass equal to the average mass and the different isotopes are distributed randomly over the lattice sites. In this case, too, the total scattering rate is equal to the sum of the individual scattering rates. In contrast to the isotopic scattering, however, the magnitude of the scattering by individual interstitial atoms or vacancies is not known. This ignorance is caused largely by the fact that it is difficult to produce interstitials or vacancies in controlled and sufficiently large num-

bers to perform thermal conductivity experiments. On the other hand, it is known from numerous studies that the phonon scattering in crystals containing substitutional foreign atoms is usually quite well described by the mass mismatch alone between the impurity and the host atom, even if charge compensation in the case of ionic crystals requires the incorporation of a vacancy or an interstitial ion together with the impurity. We refer to the work by Walker and co-workers⁶² and also to a review on doped alkali halides.²⁸ For an order-of-magnitude estimate of the average scattering rate by the single interstitial atom and the vacancy associated with it, we therefore assume that this rate is close to that caused by the missing mass alone (the mass of the displaced atom). With that assumption, we have reduced the calculation to that of the isotope effect. The missing mass causes an isotopic Rayleigh scattering with the scattering rate²⁸

$$\tau^{-1} = \Omega_0 \Gamma \omega^4 / 4 \pi v^3. \quad (4)$$

Here, Ω_0 is the volume of the individual atoms, v the sound velocity, and Γ measures the mass mismatch and the concentration of defects:

$$\Gamma = \sum_i f_i (1 - m_i / \bar{m})^2. \quad (5)$$

f_i is the fraction of the i th defect, m_i its mass, and \bar{m} is the average mass. In our case, $f_i = 1$ and $m_i = 0$, since the atom is missing. Hence we have $\Gamma = 1$ and

$$l = 4 \pi v^4 / \Omega_0 \omega^4. \quad (6)$$

For SiO_2 and GeO_2 the volume Ω_0 chosen was that of the molecules (3.76×10^{-23} and 4.95×10^{-23} cm³, respectively), since these molecules can be regarded at low temperatures as the rigid units of which the solid is formed. For Se, the atomic volume 2.92×10^{-23} cm³ was used. The mean free paths obtained from Eq. (6) have been plotted in Fig. 9, in the dominant-phonon approximation, and agree very well with the experimental values in the temperature region in which the mean free path varies as T^{-4} .

One must not take this amazingly good agreement between our model calculation and the experiment too seriously. What we believe to have shown is that the agreement is better than to within an order of magnitude. This caution seems advised for the following three reasons: (a) The dominant-phonon approximation can introduce an error of about a factor of 2, as mentioned in Sec. II. (b) In using Eq. (1) to determine the mean free path, one must use the specific heat of the plane-wave phonons. Raman scattering and far-infrared absorption measurements have been interpreted as indicating the existence of low-frequency modes of probably low group velocity,⁶³⁻⁶⁵ the excess modes referred to

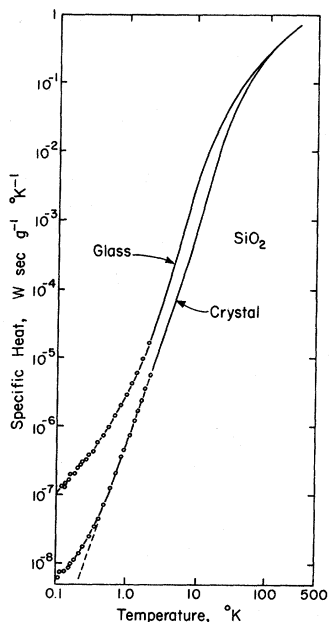


FIG. 10. Specific heat of vitreous and of crystalline SiO_2 . Our data (open circles) agree well with earlier data in the temperature region of overlap. For references see Fig. 4. The dashed line below 0.4°K marks the specific heat computed for crystalline SiO_2 from elastic measurements.

in the Introduction. In our analysis, we have, therefore, taken as C_v the specific heat of the crystalline phase, where available, namely, for SiO , SiO_2 ^{29,33,34} and Se ,³⁷⁻³⁹ although we are by no means convinced that this is the proper choice. In GeO_2 , however, only the vitreous phase has been measured.^{47,66} The lack of knowledge of the appropriate specific heat introduced a possible error estimated not to exceed a factor of 5, the maximum difference between the specific heats of vitreous and crystalline phase, for SiO_2 , and Se . (c) Finally, we should ask the fundamental question whether it is at all reasonable to describe the lattice vibrations carrying the heat in glasses with plane elastic waves having a Debye density of states in the temperature and frequency range under consideration. Equation (4) is based on this assumption. With the presently available experimental information this question cannot be answered. On the other hand, almost any fluctuation from uniform density will produce a scattering proportional $(\Delta\rho/\rho)^2$, similar in form to Eq. (4).

One of the great attractions of the isotopic model must not be forgotten among all the legitimate concerns, and that is its simplicity. It seems to be inevitable that any theory attempting to explain the experimental observations will have to be about as simple as the isotopic model in order to be equally useful for all noncrystalline solids.

To summarize, we have obtained the following remarkable result: In the temperature range above 5°K (15 cm^{-1}), the average phonon mean free path decreases as the fourth power of the temperature, and its magnitude is close to that predicted by the "isotopic" model. Above 20°K the mean free path approaches the intermolecular separation. The characteristic plateau of the conductivity of noncrystalline solids also finds a very simple explanation: The phonon mean free path decreases with increasing temperature, and finally reaches a constant value. The specific heat, on the other hand, increases with increasing temperature, and finally reaches a constant value. The plateau occurs in the temperature region in which the product of mean free path and specific heat happens to be temperature independent. According to this picture, the plateau has nothing to do with a resonance dip, and its origin is actually similar to that of the maximum in the conductivity curve of a crystal.

Below 5°K , the mean free path changes less rapidly than as T^{-4} . Below 1°K in vitreous silica and Pyrex it varies as $T^{-1.2}$. The same temperature dependence is found in vitreous Se below 0.3°K , and even the vitreous GeO_2 data appear to approach the same temperature dependence (between 0.5 and 1.2°K , the mean free path varies as $T^{-1.4}$). In their work on the polymers PS, polyvinylacetate, and PMMA, Choy *et al.* found $l \propto T^{-1.4 \pm 0.1}$ in the temperature interval $0.4 - 1.0^\circ\text{K}$.¹⁷ This behavior cannot be explained with our model. It appears as if a different scattering mechanism becomes dominant in this temperature range. Indications for this scattering have been reported before for silica-based glasses and some polymers^{9,10}: As explanation, Chang and Jones¹⁰ and Anderson *et al.*⁹ invoked phonon scattering by some internal boundaries of 10^{-2} -cm spacing. Independent evidence for such boundaries has never been reported as far as we know. Also, what kind of boundary scattering would one have to assume in order to explain such a temperature dependence of the conductivity? These questions must remain unanswered. The specific heat of glasses, to be discussed in Sec. III(B), shows an anomalous behavior below 1°K . Conceivably, a connection exists between the low-temperature anomaly and the phonon scattering at these temperatures. We will return to this point.

B. Specific Heat

We have measured the specific heat of vitreous and crystalline SiO_2 , and of vitreous GeO_2 and Se , below 1.5°K (see Figs. 10–12). Our data show a specific-heat anomaly below 1°K in all three vitreous solids. This anomaly is proportional to T in SiO_2 and GeO_2 , and, as far as one can tell from the data, also in Se . The first suspicion is that this anomaly is caused by some impurities. It has been shown by

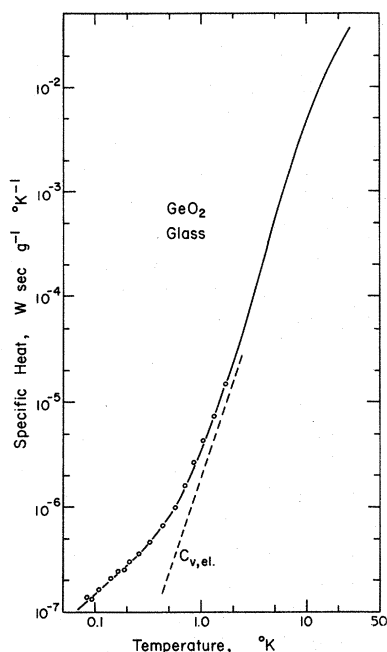


FIG. 11. Specific heat of vitreous GeO_2 . Our data (open circles) join on smoothly to the data by Wycherley (Ref. 66) above 1.4°K . The latter data, in turn, agree well with earlier data by Antoniou and Morrison (Ref. 47 and Fig. 5) except between 2 and 5°K , where Antoniou's data are up to 20% smaller than Wycherley's (see Ref. 66). The dashed line is the Debye specific heat calculated from the sound velocities in vitreous GeO_2 .

Rollefson⁵² that the motional states of F^- ions in NaBr , associated with the tunneling motion of the fluorine ion in the bromine vacancy, can cause a linear specific-heat anomaly below 1°K . This anomaly was found to scale with the fluorine concentration, and was practically absent in undoped crystals. In contrast, the anomaly in glasses seems to be quite independent of the sample, as shown in Fig. 13, where $C_v T^{-1}$ is plotted against T^2 for several samples of vitreous SiO_2 of different origins, and also in Fig. 14 for GeO_2 and Se . The anomalies are represented by the following expressions:

$$\text{SiO}_2: \Delta C_v = (1 \times 10^{-6} \text{ W sec g}^{-1} \text{ }^\circ\text{K}^{-2}) T,$$

$$\text{GeO}_2: \Delta C_v = (1.5 \times 10^{-6} \text{ W sec g}^{-1} \text{ }^\circ\text{K}^{-2}) T,$$

$$\text{Se}: \Delta C_v \approx (0.7 \times 10^{-6} \text{ W sec g}^{-1} \text{ }^\circ\text{K}^{-2}) T.$$

Note that these anomalies are comparable in magnitude to the electronic specific heat of copper, which is $C_v = (1.2 \times 10^{-5} \text{ W sec g}^{-1} \text{ }^\circ\text{K}^{-2}) T$. The most amazing fact about our anomalies is their apparent independence of the substance and accidental impurities. This suggests a common origin, conceivably the amorphous state itself. In Sec. III C, we will discuss this further.

C. Possible Origins of Specific-Heat Anomaly

We begin by comparing the low-temperature specific heat of vitreous SiO_2 with that of two samples of Pyrex glass (Fig. 15). Pyrex, too, shows an anomaly, but it does depend on the sample, and it has the shape expected for a Schottky specific-heat anomaly. It was first observed by Fisher *et al.*⁸ in Pyrex 7740 (see uppermost solid curve in Fig. 15). In a magnetic field, the anomaly shifted to higher temperatures. It was suggested that the anomaly was caused by the spins of iron impurities. This was confirmed by our results: We found that the anomaly increased with increasing iron concentration. Chemical analysis revealed 100 ppm of iron in Pyrex 7740, and 12 ppm in Pyrex 9700. From the entropy associated with the anomaly, we determined a concentration (assuming a two-level system) of 200 ppm and 50 ppm for the two glasses, in reasonable agreement with the analytic data. In vitreous silica Hornung *et al.*⁶⁷ found no change of the specific-heat anomaly in a magnetic field of 90°kG , which speaks against electronic states in this material.

Motional states of ions are another possible cause for the anomaly, since such states are quite insensitive to magnetic fields because of the large ionic mass.^{68,69} Since motional states of ions should be

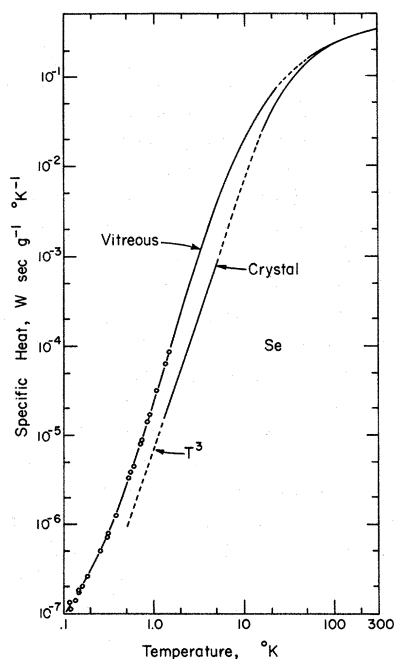


FIG. 12 Specific heat of vitreous and crystalline Se . Our data (open circles) join on smoothly to the data by Lasjaunias (Ref. 39) above 1.4°K . High-temperature data after Anderson (Ref. 37) and Desorbo (Ref. 38). The dashed lines are interpolations, drawn for clarity. Calculations of the Debye specific heat from elastic data are not available.

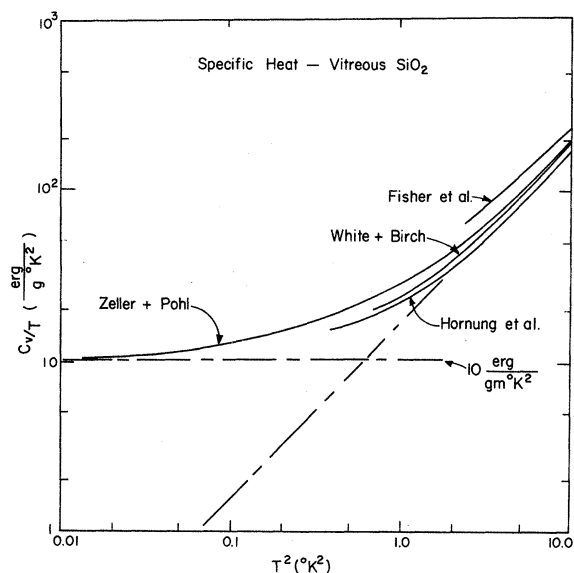


FIG. 13. Specific heat of five samples of vitreous silica, plotted as $C_v T^{-1}$ vs T^2 . The samples and their impurities, as far as known, are Flubacher *et al.* (Ref. 30, optical-quality Amersil, crushed tubing), White and Birch (Ref. 29 and private communication, I. R. Vitreosil). This material has more metallic impurities than Spectrosil B, but only about 3-ppm (by weight) hydroxyl [W. C. Dumbaugh and P. C. Schultz, *Encyclopedia of Chemical Technology*, edited by W. Kirk-Othmer (Wiley, New York, 1969), Vol. 18, p. 73], Hornung *et al.* (Ref. 66, solid cylinder of Amersil silica), Zeller (this work, Spectrosil B). According to its manufacturer Spectrosil B contains less than 0.1 ppm of Fe and Ca, less than 0.04 ppm of Na, Al, and B, less than 0.004 ppm of Ga, K, Mn, and P, and less than 0.0002 ppm of As, Sb, and Cu. It does, however, contain 0.1% hydroxyl (catalog, Thermal American Fused Quartz Co., Montville, N. J.). In spite of their different origins, the samples appear to have similar low-temperature anomalies.

expected to influence the electric polarizability, Fiory⁷⁰ measured the dielectric constant of a piece of vitreous silica cut off from one of our specific-heat samples, at temperatures above 0.1 °K, in the frequency range 10^2 – 10^4 sec⁻¹. The dielectric constant decreased with decreasing temperature, and was temperature independent below 0.5 °K to within the experimental resolution. With the assumption that the polarizable ions have dipole moments of order 1 debye (uncorrected for local fields), Fiory's measurements lead to an upper limit of 10^{16} cm⁻³ for their concentration. From the entropy associated with the specific heat, a lower limit of about $n \approx 5 \times 10^{17}$ cm⁻³ can be determined. For this analysis it was assumed that the linear specific-heat anomaly did not extend beyond approximately 1 °K, since above this temperature the rapid rise of the specific heat does not allow identification of a possible extension of the linear term any more. Hence, the

concentration could be much larger than 5×10^{17} cm⁻³. In any event, an upper limit of the dipole moment $p = 0.2$ D = $0.04e$ Å would have to be assumed in order to explain the dielectric results and the specific-heat anomaly with the motion of the same atoms. Although this is a very small dipole moment (polarizable defects in alkali halides have moments ranging between 0.3 and 6 D⁵³) it is not out of the range of what might be expected in a solid with predominantly covalent bonding. Hence, atomic motions cannot be ruled out with certainty at this point. Dielectric measurements with higher precision are under way. Fiory's observations do, however, contain strong evidence against low-lying states of electrons.

Excitations seen in specific heat below 1 °K have energies corresponding to less than 1 cm⁻¹ in the wave-number measure. Although no evidence for polarizable states was found in the kilocycle range, one might hope to see them in far-infrared optical absorption measurements. Sievers⁷¹ searched for this absorption in vitreous silica and in plexiglass (PMMA). At helium temperatures, silica was transparent (absorption constant $k < 0.04$ cm⁻¹) from $\tilde{\nu} = 4$ cm⁻¹ to the longest wavelengths studied, corresponding to $\tilde{\nu} = 1.5$ cm⁻¹. This is consistent with an extrapolation to longer wavelength of the optical absorption measured by Stolen⁶⁴ at $\tilde{\nu} > 10$ cm⁻¹ and a temperature $T = 87$ °K. In PMMA, Sievers found

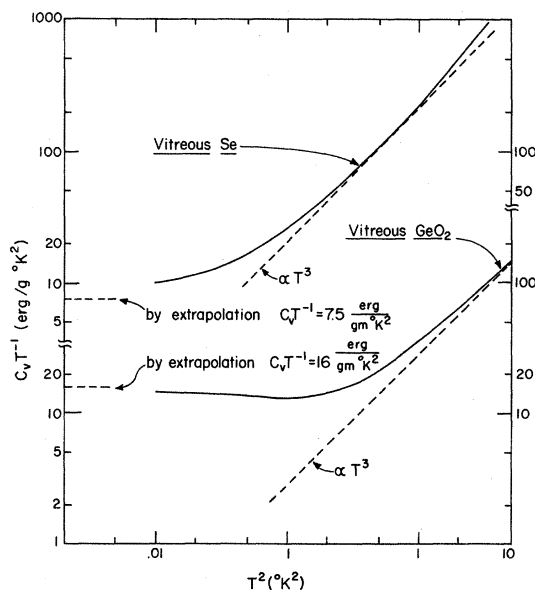


FIG. 14. Specific heat of crystalline and vitreous Se and of vitreous GeO₂, plotted as $C_v T^{-1}$ vs T^2 . Note the displaced abscissas for the two substances. The specific-heat anomalies are approximately equal for both samples, and approach a linear temperature dependence. Indications for similar anomalies were presented earlier, for PS, PMMA, and glycerol (see Fig. 5).

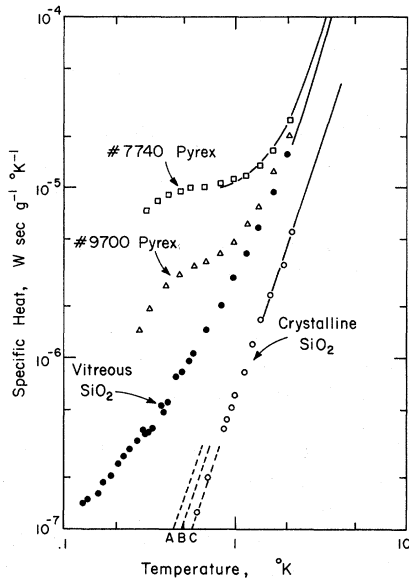


FIG. 15. Specific heat of SiO_2 and of Pyrex. Data points were obtained during present investigation; samples are listed in Table I. The solid lines are crystal SiO_2 (after Ref. 29); top curve: 7740 Pyrex (after Ref. 8); solid line just below: vitreous silica (after Ref. 30). The dashed lines are the specific heats calculated from elastic data (see Table I). A: Pyrex, $C_v = (1.14 \times 10^{-6} \text{ W sec g}^{-1} \text{ }^\circ\text{K}^{-4}) T^3$; B: vitreous SiO_2 , $C_v = (8.07 \times 10^{-7} \text{ W sec g}^{-1} \text{ }^\circ\text{K}^{-4}) T^3$; C: crystal SiO_2 , $C_v = (5.5 \times 10^{-7} \text{ W sec g}^{-1} \text{ }^\circ\text{K}^{-4}) T^3$.

$k < 0.04 \text{ cm}^{-1}$ between 1.5 and 15 cm^{-1} . Hence, these measurements also failed to give evidence for polarizable states.

At this point, the only other measurements in which the anomaly may have been observed are the thermal conductivity measurements described above. Below 1°K , the conductivity of all noncrystalline solids was found to vary with a temperature dependence close to T^2 , or $T^{1.6}$ to $T^{1.8}$, to be exact. Assume that the low-temperature specific heat of these solids contains a T^3 background whose magnitude is determined by the sound velocities in the Debye approximation, and that these Debye phonons are the only excitations which can carry heat. The mean free paths below 1°K obtained with this assumption, vary approximately as T^{-1} (see Fig. 9). If the excitations associated with the linear specific-heat anomaly act as scatterers for the plane-wave phonons, then it would be conceivable that the linear increase of the specific heat with increasing temperature would be reflected by a decrease of the phonon mean free path varying as the inverse of the temperature or close to it. With this picture, we conclude that a linear specific-heat anomaly should also exist in all other noncrystalline solids whose conductivity has been found to vary close to T^2 below 1°K . With the help of this argument we can add tentatively Pyrex and other

silica-based glasses (see Fig. 2) and also the aluminogermanate glass (Fig. 8) to the list of materials with a linear specific-heat anomaly.

In summary, all noncrystalline solids studied to date have a low-temperature specific-heat anomaly of order $10^{-6} (\text{W sec g}^{-1} \text{ }^\circ\text{K}^{-2}) T$ or show some indication for it. The excitations associated with this anomaly so far have not been influenced by dc magnetic fields and by low- and high-frequency electric fields. There is the possibility that they can scatter phonons. If these excitations are connected with atomic motion, for instance of the kind known for tunneling defects, they must have very small electric dipole moments. Conceivably, large numbers of atoms form glassy domains, tied together in the solid with weak forces, and cause excitations in the 1°K range. The linear specific-heat anomaly could also suggest one-dimensional chains. Under the arbitrary assumption that the sound velocity along these chains equals that in the bulk, it follows that about 10^{11} chains per cm^2 are needed in order to explain the magnitude of the observed anomaly.³ Because of the low frequencies involved in thermal excitations below 1°K , each chain would have to be longer than 10^3 \AA (see the scale for λ_{dom} in Fig. 9). How such linear chains, essentially decoupled from the rest of the solid, can exist in the glass is not understood.

One aspect, however, is quite clear: Any model aiming at an understanding of this anomaly has to be extremely simple in order to be equally applicable to a large number, if not to all, noncrystalline solids. Herein lies the great attraction of the problem.

ACKNOWLEDGMENTS

The first impulse to study heat transfer in glasses came from conversations with Dr. K. Dransfeld while on sabbatical leave at Cornell and with Dr. J. W. Wilkins. We want to thank them and also our colleagues R. B. Stephens, Dr. A. T. Fiory, Dr. J. A. Krumhansl, Dr. N. W. Ashcroft, and Dr. A. J. Sievers for their help and stimulating conversations. We also thank Dr. G. K. White and Dr. J. A. Birch for their permission to show their unpublished low-temperature data on vitreous silica (Fig. 13), and Dr. K. E. Wycherley and Dr. A. J. Leadbetter for informing us about their work on GeO_2 . We are very grateful to Dr. W. Dumbaugh, Dr. A. A. Erikson, and Dr. B. Wedding of the Corning Research Laboratory and to Dr. Mark Myers from the Xerox Research Laboratory for some of the samples used in this work. We also wish to thank Dr. P. J. Vergano of the Owens-Illinois Corp. for his advice regarding the preparation of the GeO_2 sample, and G. Schmidt of the Crystal Growing Laboratory of Cornell's Materials

Science Center for actually producing it. Dr. J. Roth of the Analytic Facility of the Cornell Mater-

ials Science Center performed the spectrochemical analyses on the Pyrex.

*Work supported by the U. S. Atomic Energy Commission under Contract No. At(30-1)-2391, Technical Report No. NYO-2391-130 (unpublished). Additional support was received from the Advanced Research Projects Agency through the facilities of the Materials Science Center at Cornell University, Material Science Center Report No. 1556 (unpublished). This work is part of the M. S. thesis of R. C. Zeller submitted to the Cornell Graduate School (unpublished). We also refer to this thesis for a review of the work up to 1970 on the thermal conductivity, specific heat, elastic properties, and light scattering and absorption performed on noncrystalline solids, Materials Science Center Report No. 1453 (unpublished).

†Present address: Department of Physics, Northampton County Area Community College, Bethlehem, Pa. 18017.

- ¹A. Eucken, *Ann. Physik* **34**, 185 (1911).
- ²R. Berman, *Phys. Rev.* **76**, 315 (1949).
- ³See Charles Kittel, *Introduction to Solid State Physics*, 3rd. ed. (Wiley, New York, 1966), Chap. 6.
- ⁴W. D. Seward and V. Narayanamurti, *Phys. Rev.* **148**, 463 (1966).
- ⁵R. A. Fisher, G. E. Brodale, E. W. Hornung, and W. F. Giaque, *Rev. Sci. Instr.* **40**, 365 (1969).
- ⁶E. H. Ratcliffe, *Glass Technol.* **4**, 113 (1963).
- ⁷H. E. Seeman, Ph. D. thesis (Cornell University, 1927) (unpublished).
- ⁸R. A. Fisher, G. E. Brodale, E. W. Hornung, and W. F. Giaque, *Rev. Sci. Instr.* **39**, 108 (1968).
- ⁹A. C. Anderson, W. Reese, and J. C. Wheatley, *Rev. Sci. Instr.* **34**, 1386 (1963).
- ¹⁰G. K. Chang and R. E. Jones, *Phys. Rev.* **126**, 2055 (1962).
- ¹¹R. Berman, E. L. Foster, and H. M. Rosenberg, *Brit. J. Appl. Phys.* **6**, 181 (1955).
- ¹²G. K. White, S. B. Woods, and M. T. Elford, *Phys. Rev.* **112**, 111 (1958).
- ¹³R. W. B. Stevens, *Phil Mag.* **14**, 897 (1932).
- ¹⁴R. Berman, *Proc. Roy. Soc. (London)* **A208**, 90 (1951).
- ¹⁵W. Reese, *J. Appl. Phys.* **37**, 864 (1966).
- ¹⁶K. Eiermann and K. H. Hellwege, *J. Polymer Sci.* **57**, 99 (1962); and K. Eiermann, *Kunststoffe* **51**, 512 (1961).
- ¹⁷C. L. Choy, G. L. Salinger, and Y. C. Chiang, *J. Appl. Phys.* **41**, 597 (1970).
- ¹⁸J. H. McTaggart and G. A. Slack, *Cryogenics*, **9**, 384 (1969).
- ¹⁹Kurt Guckelsberger and Jean-Claude Lasjaunias, *Compt. Rend.* **270**, B1427 (1970).
- ²⁰J. H. A. Laudy, in *Physics of Non-Crystalline Solids*, edited by J. A. Prins (North-Holland, Amsterdam, 1965).
- ²¹W. Reese and J. E. Tucker, *J. Chem. Phys.* **43**, 105 (1965).
- ²²R. L. Powell, W. M. Rogers, and D. O. Coffin, *J. Res. Natl. Bur. Std. (U.S.)* **59**, 349 (1957).
- ²³G. L. Salinger, in *Proceedings of the Third International Conference on the Physics of Noncrystalline Solids*, edited by R. W. Douglas and B. Ellis (Wiley, New York, to be published).
- ²⁴For a review, see R. C. Zeller, M. S. thesis (Cornell University, 1971) (unpublished), Cornell Materials Science Center Report No. 1453 (unpublished).
- ²⁵Charles Kittel, *Phys. Rev.* **75**, 972 (1949).
- ²⁶P. G. Klemens, *Proc. Roy. Soc. (London)* **A208**, 108 (1951).
- ²⁷P. G. Klemens, in Ref. 20, p. 162.
- ²⁸R. O. Pohl, in *Localized Excitations in Solids*, edited by R. F. Wallis (Plenum, New York, 1968), p. 434.
- ²⁹G. K. White and J. A. Birch, *Phys. Chem. Glasses* **6**, 85 (1965).
- ³⁰P. Flubacher, A. J. Leadbetter, J. A. Morrison, and B. P. Stoicheff, *J. Phys. Chem. Solids* **12**, 53 (1959).
- ³¹F. Simon, *Ann. Physik* **68**, 241 (1922).
- ³²F. Simon and F. Lange, *Z. Physik* **38**, 227 (1926).
- ³³E. F. Westrum, Jr., in *Proceedings of the Fourth International Congress on Glass, Paris, 1956* (Chaix, Paris, 1956), p. 396.
- ³⁴R. Wietzel, *Z. Anorg. Allgem. Chem.* **116**, 71 (1921).
- ³⁵O. L. Anderson, *J. Phys. Chem. Solids* **12**, 41 (1959).
- ³⁶E. F. Westrum, Jr., in *Thermodynamics and Transport Properties of Gases, Liquids and Solids* (McGraw-Hill, New York, 1959), p. 275.
- ³⁷C. T. Anderson, *J. Am. Chem. Soc.* **59**, 1036 (1937).
- ³⁸W. Desorbo, *J. Chem. Phys.* **21**, 1144 (1953).
- ³⁹Jean-Claude Lasjaunias, *Compt. Rend.* **269**, B763 (1969).
- ⁴⁰G. E. Gibson and W. F. Giaque, *J. Am. Chem. Soc.* **45**, 93 (1923).
- ⁴¹J. E. Tucker and W. Reese, *J. Chem. Phys.* **46**, 1388 (1967).
- ⁴²B. Dreyfus, N. C. Fernandes, and R. Maynard, *Phys. Letters* **A26**, 647 (1968).
- ⁴³J. C. Lasjaunias and R. Maynard, *J. Noncryst. Solids* (to be published).
- ⁴⁴J. Blanc, D. Brochter, J. C. Lasjaunias, R. Maynard, and A. Ribeyron, in *Proceedings of the Twelfth International Conference on Low Temperature Physics, Kyoto, 1970*, edited by Eizo Kanda (Academic Press of Japan, Kyoto, Japan, 1971), p. 827.
- ⁴⁵C. L. Choy, R. G. Hunt, and G. L. Salinger, *J. Chem. Phys.* **52**, 3629 (1970).
- ⁴⁶R. S. Craig, C. W. Massena, and R. M. Mallya, *J. Appl. Phys.* **36**, 108 (1965).
- ⁴⁷A. A. Antoniou and J. A. Morrison, *J. Appl. Phys.* **36**, 1873 (1965).
- ⁴⁸J. P. Harrison, *Rev. Sci. Instr.* **39**, 145 (1968).
- ⁴⁹H. S. Carslaw and J. C. Jaeger, *Conduction of Heat in Solids* (Oxford U. P., Oxford, England, 1948), Sec. 36.
- ⁵⁰R. J. Rollefson, P. P. Peressini, and C. T. Alexander, (unpublished).
- ⁵¹J. P. Harrison, G. Lombardo, and P. P. Peressini, *J. Phys. Chem. Solids* **29**, 557 (1968).
- ⁵²R. J. Rollefson, Ph. D. thesis (Cornell University, 1970) (unpublished); Cornell Materials Science Center Report No. 1382 (unpublished).
- ⁵³For a review, see V. Narayanamurti and R. O. Pohl, *Rev. Mod. Phys.* **42**, 201 (1970).
- ⁵⁴R. Q. Fugate and C. A. Swenson, *J. Appl. Phys.* **40**, 3034 (1969).
- ⁵⁵Sample kindly supplied by Dr. W. Dumbaugh, Cornell Research Center.
- ⁵⁶Performed by Dr. J. Roth, Analytical Facility, Cornell Materials Science Center.

⁵⁷Sample prepared by Dr. Mark Myers, Xerox Research Laboratory.

⁵⁸V. Garino-Canina, *J. Appl. Chem. Solids* **20**, 110 (1961).

⁵⁹P. J. Vergano and D. R. Uhlmann, *Phys. Chem. Glasses* **11**, 30 (1970).

⁶⁰J. Callaway, *Phys. Rev.* **113**, 1046 (1959).

⁶¹T. H. Geballe and G. W. Hull, *Phys. Rev.* **110**, 773 (1958).

⁶²J. A. Harrington and C. T. Walker, *Phys. Rev. B* **1**, 882 (1970); J. W. Schwartz and C. T. Walker, *Phys. Rev.* **155**, 759 (1967).

⁶³Marvin Hass, *J. Phys. Chem. Solids* **31**, 415 (1970).

⁶⁴R. H. Stolen, *J. Phys. Chem. Glasses* **11**, 83 (1970).

⁶⁵P. T. T. Wong and E. Whalley, *Trans. Faraday Soc.* (to be published).

⁶⁶K. E. Wycherley, Ph. D. thesis (School of Chemistry, University of Bristol, England, 1969) (unpublished).

⁶⁷E. W. Hornung, R. A. Fisher, G. E. Brodale, and W. F. Giauque, *J. Chem. Phys.* **50**, 4878 (1969).

⁶⁸R. A. Brand, S. A. Letzring, H. S. Sack, and W. W. Webb, *Rev. Sci. Instr.* (to be published).

⁶⁹A. T. Fiory, *Rev. Sci. Instr.* (to be published).

⁷⁰A. T. Fiory (unpublished data).

⁷¹A. J. Sievers (unpublished data).

Volume Dependence of the Grüneisen Parameter of Alkali Halides[†]

R. W. Roberts and R. Ruppin*

Department of Physics, University of North Carolina, Chapel Hill, North Carolina 27514

(Received 22 April 1971)

The parameter $q = (\partial \ln \gamma / \partial \ln V)_T$ which describes the volume variation of the Grüneisen parameter has been calculated by the following two independent methods: (a) a macroscopic calculation using a thermodynamic formula and carefully selected thermodynamic data; (b) a microscopic calculation using a six-parameter pressure-dependent lattice-dynamical shell model. The first method has been applied to twelve alkali halides and the second to only six alkali halides for which experimental data on the second-order pressure dependence of the elastic constants are available. Typical values of q have been found to be equal to about 1.5. The low-temperature limit of q has been investigated by using an acoustic-continuum model. It was found that q increases sharply at low temperatures.

I. INTRODUCTION

The parameter $q = (\partial \ln \gamma / \partial \ln V)_T$, which describes the volume dependence of the Grüneisen parameter ($\gamma = V\beta B_T / C_V$) emerges frequently in discussions of the thermoelastic properties of solids. Since no theoretical microscopic calculations of q have been performed in the past, except for a recent work on inert-gas crystals,¹ some simple assumptions about its numerical value have usually been made. Most often, q appears in relations which also involve the Anderson-Grüneisen parameters, which describe the temperature dependence of the bulk moduli and are defined by^{2,3}

$$\delta_S = -\frac{1}{\beta} \left(\frac{\partial \ln B_S}{\partial T} \right)_P, \quad (1)$$

$$\delta_T = -\frac{1}{\beta} \left(\frac{\partial \ln B_T}{\partial T} \right)_P. \quad (2)$$

Here, B_S and B_T are the adiabatic and the isothermal bulk moduli, respectively, and β is the coefficient of volume expansion. Some formulas for δ_S , which have been given in the past,⁴ were based on the assumption that $q \ll 1$, which does not hold for the alkali halides, as will be shown later. Anderson,³ on the other hand, after giving expressions for δ_S and δ_T which involve q , employed the more rea-

sonable approximation that $q = 1$. The assumption that γ is proportional to the volume (which implies $q = 1$) seems to be the most popular. It has been used in theories of shock-wave propagation⁵ and also in various discussions of equations of state.^{6,7} Another approach has been adopted by Rice⁸ in his discussion of the alkali metals. By making the assumption that the Grüneisen parameter, as well as the adiabatic bulk modulus, is a function of volume only, he was able to derive a simple explicit expression for the dependence of γ on volume. In terms of the parameter q , his relation is $q = \gamma + 1$.

A significant feature of the parameter q is that it can be calculated directly from lattice-dynamical models. A calculation of this type, based on a six-parameter shell model, is presented in Sec. III. The results are compared with q values obtained in Sec. II from room-temperature ultrasonic and thermodynamic data. The low-temperature behavior of q is discussed in Sec. IV.

II. EVALUATION OF q FROM THERMODYNAMIC AND ULTRASONIC DATA

The most convenient expression for q in terms of available experimental quantities is

$$q = 1 + (1 + T\beta\gamma)\delta_S - B'_S + \gamma + T \left(\frac{\partial \ln \gamma}{\partial T} \right)_V, \quad (3)$$